Dynamic Modeling of a Robot Manipulator for Opening the Tap Hole of an Electric Arc Furnace

Mohammad Esmaeili[1], Mohammad Saadat[1*]
[1]Department of Mechanical Engineering, Najafabad Branch, Islamic Azad University, Najafabad, Iran
[*]Email of Corresponding Author: saadat@pmc.iaun.ac.ir
Received: November 18, 2019; Accepted: February 26, 2020

Abstract
The electric arc furnace (EAF) is used to produce high quality steel from steel scraps. The EAF uses plasma arc to generate heat for melting scarp or direct reduced iron (DRI). The liquid metal should be drained from the tap hole. Manual tapping operation of the EAF in the hot environment around the furnace is a potentially dangerous and time consuming task for the workers. Therefore, it is essential to open the tap hole with Automated/robotic oxygen lancing. This study was aimed to design a robot manipulator with five degrees of freedom and revolute joints for opening the tap hole of an electrical arc furnace. The geometrical model of the robot was designed in Solid works software according to real work place and its expected path and obstacles. Direct and reverse kinematic equations were obtained using link parameters (Denawit–Hartenberg) and link transforms. The Newton-Euler approach was employed to derive the dynamic equations and the resultant joint torques.

Keywords
Electric Arc Furnace, Direct Kinematics, Inverse Kinematics, Robot Manipulator, Industrial Robot, Dynamic Model

1. Introduction

The electric arc furnace is used to provide high-quality steels form raw materials of steel scarp [1]. The electric arc furnace which is used in steelmaking was invented in 1889 by Paul He´roult. The first-generation furnaces capacity was 1 to 15 tons. In the 1960s, with the advent of billet casting, the EAF occupied another niche: it was a choice for the melting so-called mini mills. This mini mill was used for the production of rebar and wire rods [2].

In the following two decades, to decrease the tap-to-tap time required by the billet casters, the EAF reinvented itself as a melting-only unit. Steel refining was left for the recently introduced ladle furnace. Large transformers were introduced; ultrahigh-power furnaces developed, which were made possible by adopting foaming slag practice. In this way, tap-to-tap time became close to casting time. In 1985, a new niche for electric steelmaking began to be taken: flat products through thin slab casting and direct rolling. Also, this process route has achieved a significant role in world steel production. Altogether, the basic argument is that most of the ferrous scrap worldwide is recycled and refined to special steels just via electric furnaces. EAFs are versatile, charging everything from all sorts of scrap to hot briquetted iron (HBI), direct reduced iron (DRI), pig iron, hot metal. EAFs may produce all types of steels: long and flat, carbon and alloyed, for continuous casting, ingot casting, and teeming of castings in molds. Currently, EAF produces 29% of the crude steel produced worldwide (Figure 1). China, the United States, and India are the world leaders in EAF production.

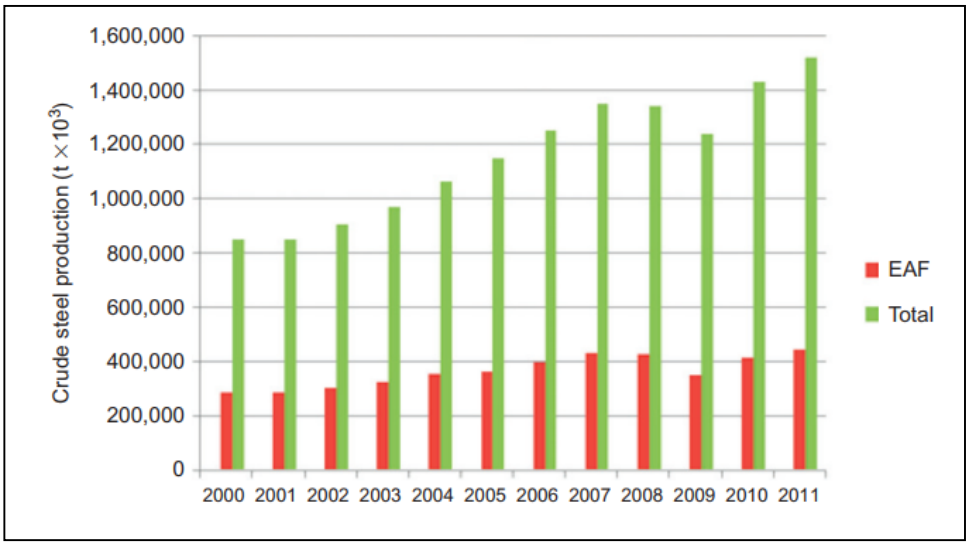

Figure1. Worldwide production of steel via EAF [2]

The electric arc furnace (EAF) uses a plasma arc to generate heat for melting scrap or direct reduced iron (DRI). The typical furnace is shown in Figure 2. It consists of a refractory-lined shell and a removable roof [1]. Electrical power is supplied to the electrodes by an adjustable voltage tap transformer and the heat by electric arcs striking between the electrodes and the scarp melts the steel [1]. The temperature of the arc column is approximately 3800°C.

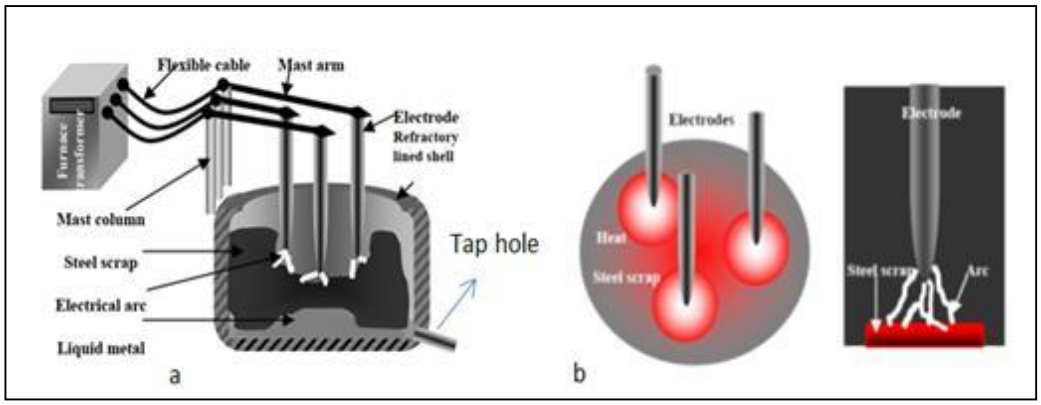

Figure2. (a) Typical electrical arc furnace. (b) Heat conversion by electric arc [1]

Manual tapping operation of the EAF in the hot environment around the furnace is a potentially dangerous and time-consuming task for the workers. There is a wide range of opening tap-hole methods, including manual oxygen lancing, Automated/robotic oxygen lancing, hydraulic drilling open, etc. Therefore, it is essential to open the tap hole with Automated/robotic oxygen lancing.
Robotics is concerned with the study of machines that can replace human beings [3]. Industrial robot manipulators are general-purpose machines used for industrial automation to increase productivity, flexibility, and product quality. Other reasons for using industrial robots are cost-saving, and elimination of hazardous and unpleasant work. Robot motion control is a key competence for robot manufacturers, and the current development is focused on increasing robot performance, reducing the

robot cost, improving safety, and introducing new functionalities. Throughout this work, the term robot was used to denote an industrial robot, i.e., a manipulator arm, mainly used for manufacturing in the industry. Some examples of such robots are shown in Figure 3 [3].

Figure3. ABB robot family [3]

Herman Hoifod investigated Dynamic Modeling and Simulation of robot manipulators by the Newton-Euler formulation. Different approaches to dynamic modeling of robot manipulators discussed, with particular focus on the Newton-Euler formulation. An automated framework for deriving the dynamic model by the Newton-Euler formulation was presented and then utilized for the IRB 140 robot [4]. Tenova melt shop, one of the world's well-known manufacturers of an electric arc furnace, recently released a video showing a robot manipulator with 5 degrees of freedom to sample melting [5]. Danieli Group Company, one of the world well-known manufactures of EAF, designed robots which Q-named (Figure 4), divided into three groups: (i) Q-robot melt sample for melt sampling and temperature measurement, (ii) Q-Robot melt EBT to open tap hole of EBT, (iii) Q-Robot melt scan for thickness measurement of refractory materials and 3-D modeling [6].

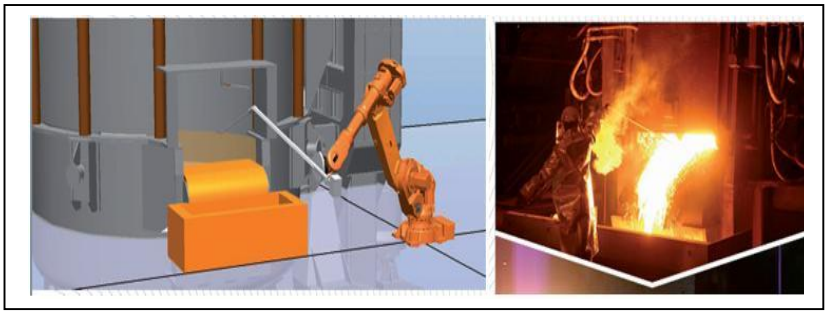

Figure4. Q-Robot melt sample [6]

The process of opening the tap hole of an electric arc furnace is performed by the operator which is very dangerous due to possible injuries. Therefore, it is necessary to design a robot manipulator to work in this situation. Besides, in some melting operations, the time of opening the tap hole is very long which leads to decreasing the productivity of the furnace.

Throughout this study, a robot manipulator with 5 degrees of freedom was designed for opening the tap hole of a real electric arc furnace and thereafter, the complete dynamic model of robot was derived by the Newton-Euler formulation. Finally, kinematic and dynamic equations were derived.

2. Methodology

The Denawit – Hartenberg method used to model the mechanism of the designed robot. In this method, local coordinate frames were attached to the links precisely. Figure 5 gives a clear view of the manipulator and its degrees of freedom. The manipulator has five revolute joints.

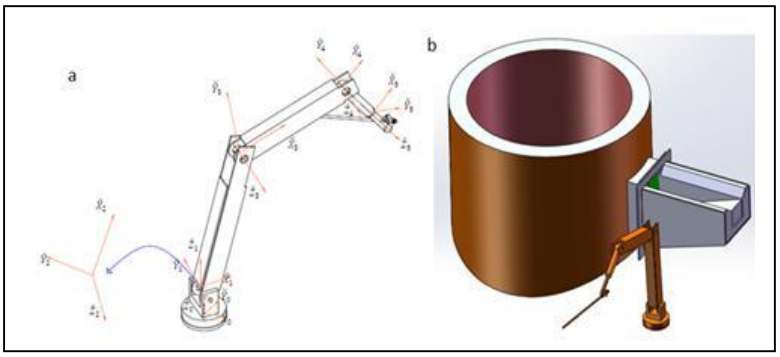

Figure5. (a) Robot manipulator with 5 degrees of freedom. (b). shell and tap hole of EAF

The Denawit–Hartenberg parameters (link parameters), describing the geometry and relative displacement, are shown in Table 1. Rotation matrixes and homogeneous transforms could be calculated using link parameters. The position and orientation of the robot joints were specified with rotation matrixes and Homogeneous transforms.

Table1. Links parameters

Joint number	α_{i-1}	a_{i-1}	d_i	θ_i
1	0	0	0.3 m	θ_1
2	90	0	0	θ_2
3	0	1.175 m	0	θ_3
4	0	1.37 m	0	θ_4
5	90	0	0.52 m	θ_5

To obtain direct kinematics of a robot manipulator, one should define the homogenous transforms matrix for each joint [7]. Using DH parameters, the homogenous transformation matrix for a single joint is expresses as Equation 1.

$$ {}^{i-1}_{i}T = \begin{bmatrix} \cos\theta_i & -\sin\theta_i & 0 & a_{i-1} \\ \sin\theta_i\cos\alpha_{i-1} & \cos\theta_i\cos\alpha_{i-1} & -\sin\alpha_{i-1} & -d_i\sin\alpha_{i-1} \\ \sin\theta_i\sin\alpha_{i-1} & \cos\theta_i\sin\alpha_{i-1} & \cos\alpha_{i-1} & d_i\cos\alpha_{i-1} \\ 0 & 0 & 0 & 1 \end{bmatrix} \quad (1) $$

Transformation matrices for the 5 DOF robots are given as:

$$ {}^{0}_{1}T = \begin{bmatrix} \cos\theta_1 & -\sin\theta_1 & 0 & 0 \\ \sin\theta_1 & \cos\theta_1 & 0 & 0 \\ 0 & 0 & 1 & 0.3 \\ 0 & 0 & 0 & 1 \end{bmatrix} \quad (2) $$

$$ {}^{1}_{2}T = \begin{bmatrix} \cos\theta_2 & -\sin\theta_2 & 0 & 0 \\ 0 & 0 & -1 & 0 \\ \sin\theta_2 & \cos\theta_2 & 0 & 0 \\ 0 & 0 & 0 & 1 \end{bmatrix} \quad (3) $$

$$ {}^{2}_{3}\mathrm{T} = \begin{bmatrix} \cos\theta_3 & -\sin\theta_3 & 0 & 1.75 \\ \sin\theta_3 & \cos\theta_3 & 0 & 0 \\ 0 & 0 & 1 & 0 \\ 0 & 0 & 0 & 1 \end{bmatrix} \quad (4) $$

$$ {}^{3}_{4}\mathrm{T} = \begin{bmatrix} \cos\theta_4 & -\sin\theta_4 & 0 & 1.37 \\ \sin\theta_4 & \cos\theta_4 & 0 & 0 \\ 0 & 0 & 1 & 0 \\ 0 & 0 & 0 & 1 \end{bmatrix} \quad (5) $$

$$ {}^{4}_{5}\mathrm{T} = \begin{bmatrix} \cos\theta_5 & -\sin\theta_5 & 0 & 0 \\ 0 & 0 & -1 & -0.52 \\ \sin\theta_5 & \cos\theta_5 & 0 & 0 \\ 0 & 0 & 0 & 1 \end{bmatrix} \quad (6) $$

Once the link frames had been defined and the corresponding link parameters found, developing the kinematic equations was straightforward. From the values of the link parameters, the individual link-transformation matrices could be computed. Then the link transformations could be multiplied together to find the single transformation that relates frame {5} to frame {0}:

$$ {}^{0}_{5}\mathrm{T} = {}^{0}_{1}\mathrm{T}\,{}^{1}_{2}\mathrm{T}\,{}^{2}_{3}\mathrm{T}\,{}^{3}_{4}\mathrm{T}\,{}^{4}_{5}\mathrm{T} = \begin{bmatrix} r_{11} & r_{12} & r_{13} & P_x \\ r_{21} & r_{22} & r_{23} & P_y \\ r_{31} & r_{32} & r_{33} & P_z \\ 0 & 0 & 0 & 1 \end{bmatrix} \quad (7) $$

$$ r_{11} = \cos\theta_1\cos\theta_5\cos(\theta_2+\theta_3+\theta_4) + \sin\theta_1\sin\theta_5 \quad (8) $$

$$ r_{21} = \sin\theta_1\cos\theta_5\cos(\theta_2+\theta_3+\theta_4) - \cos\theta_1\sin\theta_5 \quad (9) $$

$$ r_{31} = \cos\theta_5\sin(\theta_2+\theta_3+\theta_4) \quad (10) $$

$$ r_{41} = 0 \quad (11) $$

$$ r_{12} = -\cos\theta_1\sin\theta_5\cos(\theta_2+\theta_3+\theta_4) + \sin\theta_1\cos\theta_5 \quad (12) $$

$$ r_{22} = -\sin\theta_1\sin\theta_5\cos\big(\theta_2+\theta_3+\theta_4\big) - \cos\theta_1\cos\theta_5 \quad (13) $$

$$ r_{32} = -\sin\theta_5\sin(\theta_2+\theta_3+\theta_4) \quad (14) $$

$$ r_{42} = 0 \quad (15) $$

$$ r_{13} = \cos\theta_1\sin(\theta_2+\theta_3+\theta_4) \quad (16) $$

$$ r_{23} = \sin\theta_1\sin(\theta_2+\theta_3+\theta_4) \quad (17) $$

$$ r_{33} = \cos(\theta_2+\theta_3+\theta_4) \quad (18) $$

$$ r_{43} = 0 \quad (19) $$

$$ P_x = \cos\theta_1\big(\cos\theta_2(d_5\sin(\theta_3+\theta_4) + a_3\cos\theta_3 + a_2) - \sin\theta_2(-d_5\cos(\theta_3+\theta_4) + a_3\sin\theta_3)\big) \quad (20) $$

$$ P_y = \sin\theta_1\big(\cos\theta_2(d_5\sin(\theta_3+\theta_4) + a_3\cos\theta_3 + a_2) - \sin\theta_2(-d_5\cos(\theta_3+\theta_4) + a_3\sin\theta_3)\big) \quad (21) $$

$$ P_z = \sin\theta_2(d_5\sin(\theta_3+\theta_4) + 1.37\cos\theta_3 + 1.75) + \cos\theta_2(-d_5\cos(\theta_3+\theta_4) + 1.37\sin\theta_3) + 0.3 \quad (22) $$

$$r_{44} = 1 \tag{23}$$

The mentioned equations constituted the kinematics of the robot. They specify how to compute the position and orientation of frame {5} relative to frame {0} of the robot. These are the basic equations for all kinematic analysis of this manipulator.
Joint angles of the robot at their initial position which extracted from SOLIDWORKS software were substituted in the kinetic equations for validity. This can be also proved from Figure6 in which similar results in terms of the position of joints were obtained from SOLIDWORKS and Matlab code.

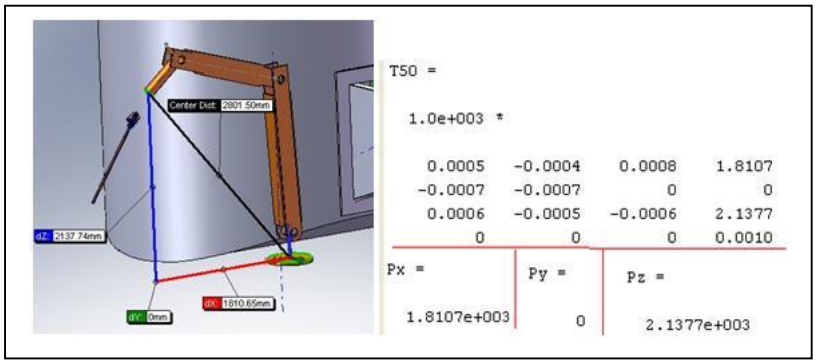

Figure6. The validity of kinematics equations

Unlike the direct kinematic, in inverse kinematic by given the desired position and orientation of the robot, the joints angles were computed. The problem of solving the inverse kinematic equations of the robot was a nonlinear one. There are no general algorithms that may be employed to solve nonlinear equations. The solution of the inverse kinematics problem is computationally expensive and generally takes much time for real-time control of robot manipulators. It is very important for robot design, trajectory planning and dynamic analysis of robot manipulators. There are mainly two types of inverse kinematics solutions techniques, namely analytical and numerical.
Given the numerical value of ${}^{0}_{5}\mathrm{T}$, the goal is to solve Equation 7.

$$\theta_1 = \mathrm{Arctan2}\left(P_y, P_x\right) \tag{24}$$

$$P_x\cos\theta_1 + P_y\sin\theta_1 = 0.52\sin(\theta_2+\theta_3+\theta_4) + 1.37\cos(\theta_2+\theta_3) + 1.75\cos\theta_2 \tag{25}$$

$$P_z - 0.3 = -0.52\cos(\theta_2+\theta_3+\theta_4) + 1.37\sin(\theta_2+\theta_3) + 1.75\sin\theta_2 \tag{26}$$

$$\cos(\theta_2+\theta_3+\theta_4) = 0 \tag{27}$$

$$\begin{aligned}(\cos\theta_1\cos(\theta_3+\theta_4) - \cos\theta_1\sin\theta_2\sin(\theta_3+\theta_4))\cos\theta_1\sin(\theta_2+\theta_3+\theta_4)\\ + \sin\theta_1\cos(\theta_2+\theta_3+\theta_4)\sin\theta_1\sin(\theta_2+\theta_3+\theta_4)\\ + \sin(\theta_2+\theta_3+\theta_4)\cos(\theta_2+\theta_3+\theta_4)\\ = \cos\theta_5\end{aligned} \tag{28}$$

The Newton-Euler formulation was used for the derivation of dynamic equations of motion of the robot. This method is based on a balance of all forces acting on the generic link of the manipulator.

The complete algorithm for computing dynamic equation from the motion of the joints is composed of two parts. First, link velocities and accelerations are iteratively computed from link 1 out to link 5 and the Newton—Euler equations were applied to each link. Second, forces and torques of interaction and joint actuator torques are computed recursively from link 5 back to link 1. The equations are summarized next for the case of all joints rotational:

$$\mathrm{i}: 0 \to 5 \tag{29}$$

$${}^{i+1}\omega_{i+1} = {}^{i+1}_{i}R\,{}^{i}\omega_i + \dot{\theta}_{i+1}\,{}^{i+1}\hat{Z}_{i+1} \tag{30}$$

$${}^{i+1}v_{i+1} = {}^{i+1}_{i}R\left({}^{i}v_i + {}^{i}\omega_i \times {}^{i}P_{i+1}\right) \tag{31}$$

$${}^{i+1}\dot{\omega}_{i+1} = {}^{i+1}_{i}R\,{}^{i}\dot{\omega}_i + {}^{i+1}_{i}R\,{}^{i}\omega_i \times \dot{\theta}_{i+1}\,{}^{i+1}\hat{Z}_{i+1} + \ddot{\theta}_{i+1}\hat{Z}_{i+1} \tag{32}$$

$${}^{i+1}\dot{v}_{i+1} = {}^{i+1}_{i}R\left({}^{i}\dot{\omega}_i \times {}^{i}P_{i+1} + {}^{i}\omega_i \times \left({}^{i}\omega_i \times {}^{i}P_{i+1}\right) + {}^{i}\dot{v}_i\right) \tag{33}$$

$${}^{i+1}\dot{v}_{C_{i+1}} = {}^{i+1}\dot{\omega}_{i+1} \times {}^{i+1}P_{C_{i+1}} + {}^{i+1}\omega_{i+1} \times \left({}^{i+1}\omega_{i+1} \times {}^{i+1}P_{C_{i+1}}\right) + {}^{i+1}\dot{v}_{i+1} \tag{34}$$

$${}^{1}\dot{v}_{c_1} = {}^{1}\dot{\omega}_1 \times {}^{1}P_{C_1} + {}^{1}\omega_1 \times \left({}^{1}\omega_1 \times {}^{1}P_{C_1}\right) + {}^{1}\dot{v}_1 \tag{35}$$

$$\mathrm{i}: 6 \to 1 \tag{36}$$

$${}^{i+1}F_{i+1} = m_{i+1}\,{}^{i+1}\dot{v}_{C_{i+1}} \tag{37}$$

$${}^{i+1}N_{i+1} = {}^{C_{i+1}}I_{i+1}\,{}^{i+1}\dot{\omega}_{i+1} + {}^{i+1}\omega_{i+1} \times {}^{C_{i+1}}I_{i+1}\,{}^{i+1}\omega_{i+1} \tag{38}$$

$${}^{i}f_i = {}^{i}_{i+1}R\,{}^{i+1}f_{i+1} + {}^{i}F_i \tag{39}$$

$${}^{i}n_i = {}^{i}N_i + {}^{i}_{i+1}R\,{}^{i+1}n_{i+1} + {}^{i}P_{C_i} \times {}^{i}F_i + {}^{i}P_{i+1} \times {}^{i}_{i+1}R\,{}^{i+1}f_{i+1} \tag{40}$$

$${}^{i}\tau_i = {}^{i}n_i{}^{T}\hat{Z}_i \tag{41}$$

Extracting $\hat{Z}$ the components of the ${}^{i}n_i$, joint torques $\tau_1, \tau_2, \tau_3, \tau_4$ and $\tau_5$were obtained. Equations give an expression for the torque at the actuators as a function of joint position, velocity, and acceleration. Not that these quite complex function arose from 5 degrees of freedom. When the Newton—Euler equations are evaluated symbolically for any manipulator, they yield a dynamic equation that can be written in the form

$$\tau = M(\Theta)\ddot{\Theta} + V\left(\Theta, \dot{\Theta}\right) + G(\Theta) \tag{42}$$

Where, $M(\Theta)$ is the 5×5 mass matrix of the manipulator, $V(\Theta, \dot{\Theta})$ is a 5×1 vector of centrifugal and Coriolis terms, and $G(\Theta)$ is a 5×1vector of gravity terms. Each element of $M(\Theta)$ and $G(\Theta)$ is a complete function that depends on Θ, the position of all the joints of the manipulator. Each element of $V(\Theta, \dot{\Theta})$ is a complex function of both Θ and $\dot{\Theta}$.

Equation (42) gives expressions for the torque at the actuators as a function of joint position, velocity, and acceleration. Obviously, the closed-form equations for a manipulator with six degrees of freedom will be quite complex.

3. Conclusion

The critical importance of robot manipulator for opening the tap hole of EAF and management to furnace performance and increase safety was demonstrated. In a manual opening tap hole, the operators always exposed to high risk and dangerous situations such as lot liquid, hot lining, environmental contaminant ant tapping system, so a fully automated and remote device such as a robot manipulator is required.

The basic mathematical tools used in the study of the kinematics of the robot were introduced. The link parameters d_i, θ_i, a_i and α_i was achieved. Rotation matrix and homogenous transforms were obtained, which describe the position and orientation of the robot's link. The homogenous transformation matrix leads to a compact formulation of the kinematics equations. The direct and inverse kinematics problems were formulated. It was shown that the direct kinematics problem was relatively simple to solve, while the inverse kinematics problem includes difficulties with the existence of a real solution, with multiple solutions and with a convergence of iterative numerical procedures. Finally, the dynamic equation was derived based on the Newton – Euler approach.

4. References

[1] Labar, H., Djeghader, Y., Samira, K. M. and Kamel, B. 2009. Closely parametrical model for an electrical arc furnace. World Academy of Science. Engineering and Technology. 40: 96-100.

[2] Seetharaman, S., Mclean, A. and Goodwill, J. E. 2014. Treatise on process metallurgy: industrial processes. Royal Institute of Technology. Stockholm, Sweden.

[3] Moberg, S. 2010. Modeling and control of flexible manipulators. Ph.D. Thesis. Department of Electrical Engineering Linköping University, SE–581 83 Linköping, Sweden.

[4] Høifødt, H. 2011. Dynamic modeling and simulation of robot manipulators. MSc Thesis, Department of Engineering Cybernetics. Norwegian University of Science and Technology.

[5] Tenova. 2015. Melt shops top charge EAF with a anthropomorphic temperature and sampling Robot. URL: https://www.youtube.com/watch?v=7Yr5qYZUpso.

[6] Danieli, Q-Robot Melt Anthropomorphic robot for temperature sampling and steel Analysis in EAF's. URL:https://www.dca.it/media/download/brochure-q-robot-melt.pdf.

[7] Kucuk, S. and Bingul, A. 2005. The inverse kinematics solutions of fundamental robot manipulators with offset wrist. Proceeding of the IEEE ICM/HIMA. Taiwan, 197-202.